Role of Microstructure in Promoting Fracture and Fatigue Resistance in Mo-Si-B Alloys

J. J. Kruzic*
Department of Mechanical Engineering, Oregon State University, Corvallis, OR 97331, U.S.A.
J. H. Schneibel
Oak Ridge National Laboratory, Metals and Ceramics Division, Oak Ridge, TN 37831, U.S.A.
R. O. Ritchie
Department of Materials Science and Engineering, University of California, and Materials Sciences Division, Lawrence Berkeley National Laboratory, Berkeley, CA 94720, U.S.A.

ABSTRACT

An investigation of how microstructural features affect the fracture and fatigue properties of a promising class of high temperature Mo-Si-B based alloys is presented. Fracture toughness and fatigue-crack growth properties are measured at 25º and 1300ºC for five Mo-Mo_3Si-Mo_5SiB_2 containing alloys produced by powder metallurgy with α-Mo matrices. Results are compared with previous studies on intermetallic-matrix microstructures in alloys with similar compositions. It is found that increasing the α-Mo phase volume fraction (17 – 49%) or ductility (by increasing the temperature) benefits the fracture resistance; in addition, α-Mo matrix materials show significant improvements over intermetallic-matrix alloys. Fatigue thresholds were also increased with increasing α-Mo phase content, until a transition to more ductile fatigue behavior occurred with large amounts of α-Mo phase (49%) and ductility (i.e., at 1300°C). The beneficial role of such microstructural variables are attributed to the promotion of the observed toughening mechanisms of crack trapping and bridging by the relatively ductile α-Mo phase.

INTRODUCTION

Intermetallic based Mo-Si-B alloys have been targeted for high temperature turbine engine applications as potential replacements for nickel based superalloys. Two specific Mo-Si-B alloy systems developed by Akinc *et al.* [1-4] and Berczik [5,6] have received recent attention. While the former is composed entirely of intermetallic compounds, the latter utilizes the relatively ductile α-Mo phase to impart some ductility and fracture resistance to a three phase microstructure also containing Mo_3Si and Mo_5SiB_2 (T2). For any of these alloys to be successful, adequate resistance to oxidation, creep, fracture, and fatigue must be achieved; however, it is recognized that microstructural features which promote improvements in one property are often detrimental to others [7,8]. For example, while a continuous α-Mo matrix with high volume fraction may be beneficial to the fracture and fatigue behavior [9], this tends to compromise the oxidation and creep resistance [7,8,10-12]. Accordingly, a thorough understanding of how microstructure affects each property is needed so that appropriate trade-offs can be made in the optimization of these alloys. Consequently, this present paper seeks to characterize the specific mechanistic role of microstructure in determining the fracture and fatigue resistance of alloys based on the α-Mo, Mo_3Si, and T2 phases, with the objective of

* Corresponding author. Tel: +1-541-737-7027; fax: +1-541-737-2600.
E-mail address: jamie.kruzic@oregonstate.edu (J. J. Kruzic)

providing guidelines for optimizing the properties of this exciting new class of high-temperature structural materials.

EXPERIMENTAL DETAILS

Ground powders of composition Mo-20Si-10B (at.%) containing Mo_3Si (cubic A15 structure) and Mo_5SiB_2 (tetragonal $D8_1$ structure) intermetallic phases were vacuum-annealed to remove silicon from the surface and leave an α-Mo coating on each particle. These were hot-isostatically pressed in evacuated Nb cans for 4 hr at 1600°C and 200 MPa pressure giving final compositions with 7-15 at.% Si and 8-11 at.% B (balance Mo). Five alloys were produced differing in volume fraction of the α-Mo matrix (17 – 49%) and initial coarseness of the intermetallic particles, fine ≤45 μm, medium 45-90 μm, and coarse 90-180 μm. Alloys are designated as F34, M34, C17, C46, and C49, with the letter indicating the microstructural coarseness and the number giving the α-Mo volume percent; microstructures for each may be seen in Figures 1 and 2.

Resistance-curve (R-curve) fracture-toughness experiments were performed on fatigue pre-cracked, disk-shaped compact-tension DC(T) specimens (width 14 mm; thickness 3 mm). Samples were loaded monotonically in displacement control at ~1 μm/min until the onset of cracking. At 25°C, periodic unloads (~10-20% of peak load) were performed to measure the unloading back-face strain compliance, which was used to determine the crack length [13]. 1300°C tests were conducted in gettered argon using (direct-current) electrical potential-drop techniques to monitor crack length [14].

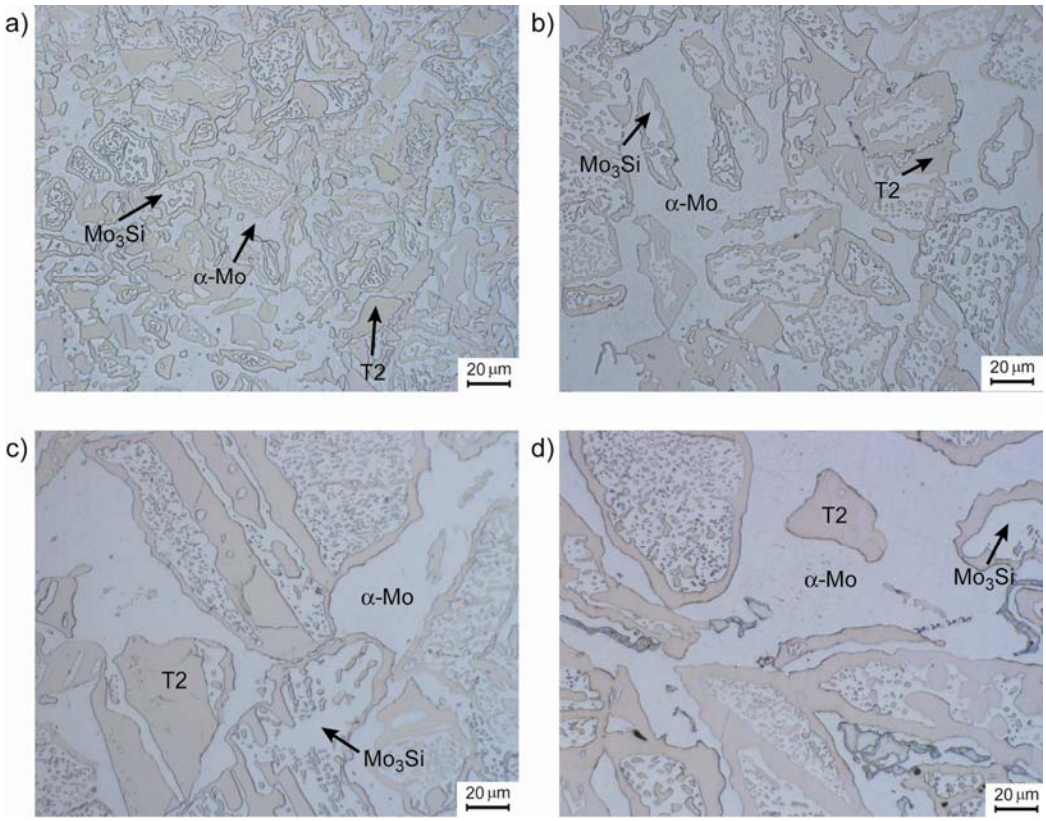

Figure 1. Microstructures of alloys (a) F34, (b) M34, (c) C17, and (d) C46. (C49 is seen in Figure 2b)

Fatigue-crack growth testing (25 Hz, sine waveform) was performed at 25° and 1300°C in identical environments in general accordance with ASTM Standard E647 [15] using computer-controlled servo-hydraulic testing machines at a load ratio R (ratio of minimum to maximum loads) of 0.1. Crack-growth rates, da/dN, were determined as a function of the stress-intensity range, ΔK, using continuous load-shedding to maintain a ΔK-gradient (=$1/\Delta K[d\Delta K/da]$) of ±0.08 mm^{-1} to achieve increasing or decreasing ΔK conditions, respectively. ΔK_{TH} fatigue thresholds, operationally defined at a minimum growth rate of 10^{-10}–10^{-11} m/cycle, were approached under decreasing ΔK conditions. Both fracture and fatigue testing was periodically paused to observe crack profiles using optical and scanning electron microscopy.

RESULTS AND DISCUSSION

R-curves for the five Mo-Mo_3Si-T2 alloys are plotted in terms of the stress intensity, K, and clearly indicate rising fracture toughness with crack extension (Figure 2a). Furthermore, there is a trend of increasing toughness with higher α-Mo volume fractions; indeed, alloys C46 and C49 had peak room-temperature toughnesses in excess of 20 MPa√m, i.e., up to seven times higher than that of monolithic molybdenum silicides [16,17]. Crack trapping and bridging by the α-Mo phase were identified as the toughening mechanisms responsible for this behavior (Figure 2b), with the effectiveness of these mechanisms rising with increasing α-Mo content. Experiments at 1300ºC on alloys M34, C17, and C46 indicated that the fracture toughness improved at higher temperatures, which was associated with improved α-Mo ductility. The initiation toughness, K_i, which defines the beginning of the R-curve, rose ~65% for alloys M34 and C17, while alloy C46 experienced toughening at 1300ºC to such a degree that large-scale crack blunting and deformation occurred (Figure 3a) and linear-elastic fracture mechanics was no longer a valid method for assessing the toughness using the present specimen size. Thus, K_i for alloy C46 at 1300ºC is reasoned to be significantly larger than the 12.6 MPa√m measured for alloy M34.

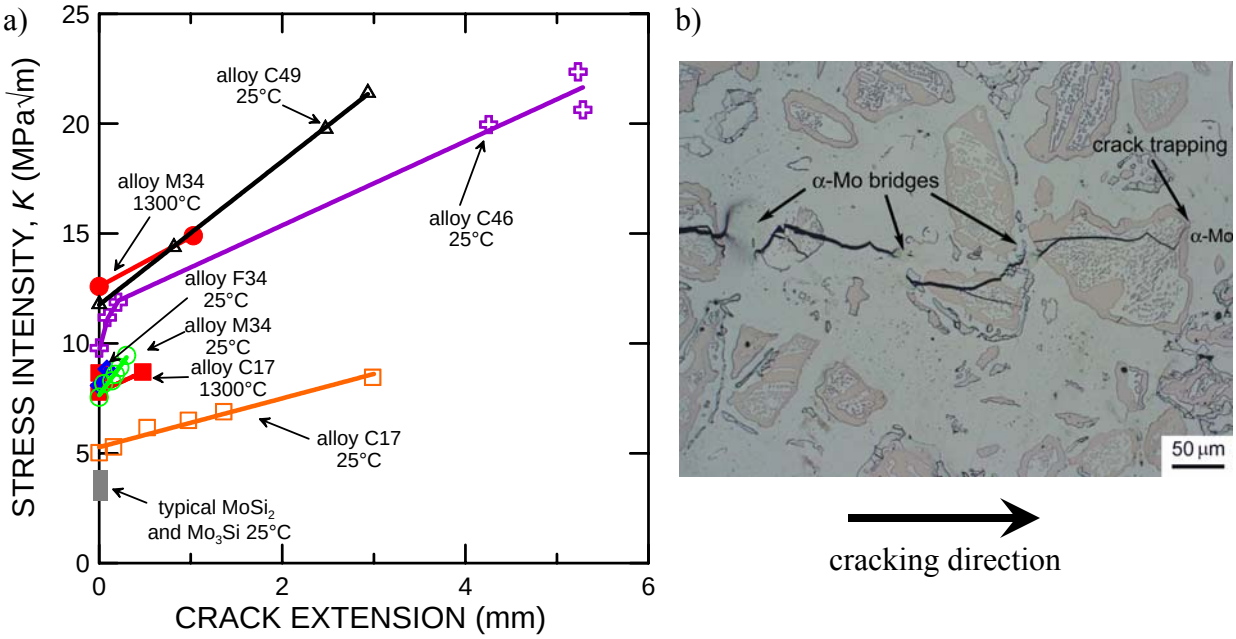

Figure 2. (a) shows R-curve behavior for Mo-Si-B alloys, while (b) shows the active toughening mechanisms, crack trapping and bridging by the α-Mo phase of alloy C49.

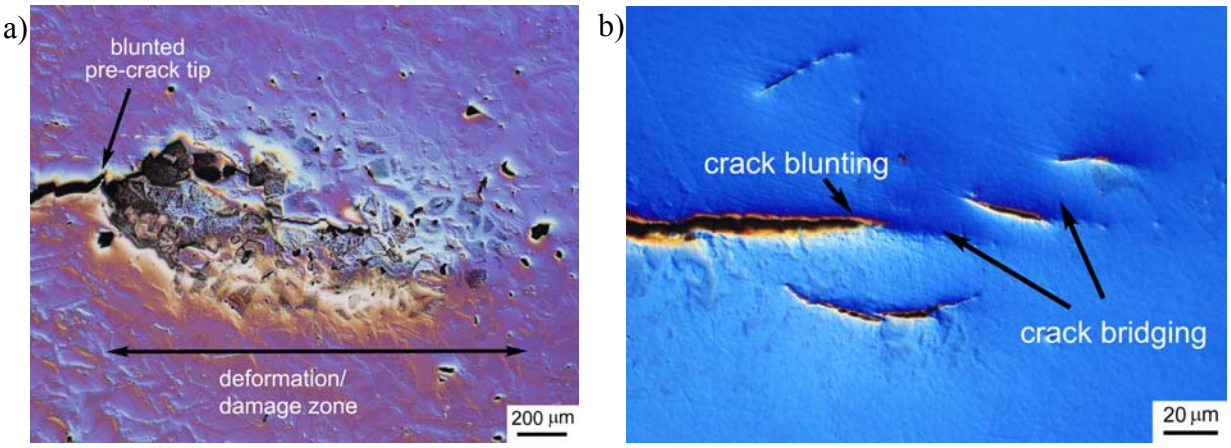

Figure 3. Crack blunting seen in alloys (a) C46 and (b) M34 after R-curve testing at 1300°C. Note the order of magnitude difference in scale between the two micrographs.

Crack blunting was also observed, to a much smaller degree, in the other alloys tested at 1300ºC (Figure 3b). Thus, increases in toughness with temperature were attributed to the improved effectiveness of crack trapping due to the enhanced α-Mo ductility at elevated temperatures.

From the fatigue-crack growth results in Figure 4a, it is apparent that at 25ºC the Paris-law exponents, *m*, are extremely high, >78 in all cases; such behavior is characteristic of brittle materials. Fatigue data were also collected for alloys M34 and C49 at 1300°C; although alloy M34 had a similarly high Δ*K* dependence at 1300ºC, alloy C49 displayed a transition to more ductile fatigue behavior, with more than an order of magnitude decrease in the Paris-law exponent from 78 to 4. A Paris exponent of 4 is similar to what is expected for ductile metals, which typically have $m = 2 - 4$ [18]. ΔK_{TH} thresholds ranged between 5 and 9.5 MPa√m for the five alloys at 25°C (Figure 4a). At 1300°C, due to experimental difficulties and limited numbers of samples, data were not collected near the operationally-defined fatigue threshold; however,

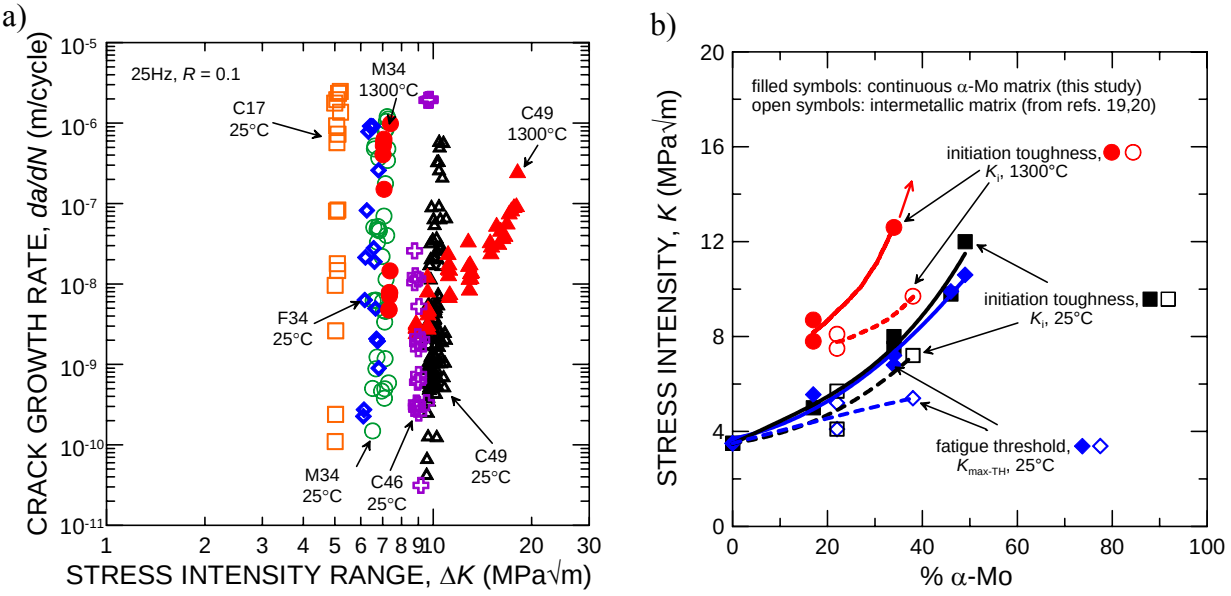

Figure 4. Plots showing (a) the fatigue-crack growth behavior for present alloys, and (b) the fracture toughness and fatigue threshold properties of the present α-Mo matrix alloys compared to that for intermetallic-matrix alloys of similar compositions from refs. [19,20].

based on extrapolation of the data in Figure 4a, the threshold for M34 is expected to be similar to that at 25°C, whereas data for alloy C49 suggests a decrease in the fatigue threshold at 1300°C.

Figure 4b compiles the present fracture and fatigue results along with those for intermetallic matrix Mo-Si-B alloys with similar compositions [19,20]. Here the fatigue thresholds are plotted as the maximum stress intensity, $K_{max,TH}$, along with the initiation toughness values, K_i. Peak toughnesses are not compared since steady-state, or plateau, values were not achieved due to inadvertent failure of specimens and/or limited specimen size. Figure 4b clearly illustrates that the fracture and fatigue properties of all the alloys improve with increasing α-Mo volume fraction. Furthermore, the fracture toughness properties are enhanced with increasing α-Mo ductility, as evidenced by the higher toughness values at 1300°C for all the alloys. Note that a given toughness value may be achieved with lower α-Mo volume fraction if the ductility of the α-Mo can be improved; in the present work, this is accomplished by increasing the temperature. If the room temperature ductility of α-Mo phase can be improved by compositional or microstructural means, lower α-Mo volume fractions will be needed to achieve adequate toughness levels; this is important since the α-Mo phase compromises the oxidation and creep resistance [7,8,10-12] and thus its volume fraction should be minimized if possible.

The fracture and fatigue properties of the present α-Mo matrix materials are also superior to those of the intermetallic-matrix Mo-Si-B alloys [19,20]. This is attributed to higher effectiveness of the crack trapping and bridging mechanisms when there is a continuous α-Mo matrix, since the crack cannot avoid the relatively ductile phase. Furthermore, this effect is enhanced when either the α-Mo volume fraction or ductility (e.g., at 1300°C) is increased, indicating that these factors do not affect the mechanical behavior independently. Finally, alloys with coarser microstructural size-scales demonstrated slightly improved fracture toughness and fatigue properties. This may be seen in the improved crack stability for alloy C17 relative to the tougher alloys F34 and M34. Although F34 and M34 were tougher due to higher α-Mo volume fractions, stable crack growth was more easily accomplished in alloy C17, allowing the collection of R-curve data over several millimeters without catastrophic failure. Similar improved crack stability was also observed during fatigue testing of the coarser microstructures.

CONCLUSIONS

Based on an experimental study of ambient- to high-temperature fracture toughness and fatigue-crack propagation behavior in five Mo-Si-B alloys, containing Mo_3Si and Mo_5SiB_2 intermetallic phases dispersed within a continuous α-Mo matrix, the following conclusions are made:

1. α-Mo matrix Mo-Si-B alloys exhibit far superior fracture and fatigue resistance relative to unreinforced silicides, with fracture toughnesses in excess of 20 MPa√m for α-Mo volume fractions > 45%. Such gains are attributed to crack trapping and crack bridging by the α-Mo phase.
2. Higher α-Mo volume fractions benefited both of these mechanisms, leading to improved fracture and fatigue resistance. Furthermore, the fracture resistance was improved at 1300°C, indicating the role that α-Mo ductility plays in determining mechanical properties. Finally, a given level of fracture resistance may be achieved with lower α-Mo volume fraction by improving α-Mo ductility, a desirable feature since α-Mo compromises the oxidation and creep resistance.

3. Using a continuous α-Mo matrix instead of an intermetallic matrix is also beneficial for the fracture toughness and fatigue-crack growth properties. However, larger beneficial effects are found by increasing the α-Mo volume fraction and ductility. Additionally, coarser microstructures promote fracture and fatigue resistance, specifically by aiding crack bridging and stability.

ACKNOLEDGEMENTS

This work was supported by the Office of Fossil Energy, Advanced Research Materials Program, WBS Element LBNL-2, and by the Office of Science, Office of Basic Energy Sciences, Division of Materials Sciences and Engineering of the U.S. Department of Energy, under contract DE-AC03-76SF0098 with the Lawrence Berkeley National Laboratory for ROR and JJK. JHS acknowledges funding of this work by the Office of Fossil Energy, Advanced Research Materials (ARM) Program, WBS Element ORNL-2(I), and by the Division of Materials Sciences and Engineering, U.S. Department of Energy, under contract DE-AC05-00OR22725 with Oak Ridge National Laboratory managed by UT-Battelle.

REFERENCES

1. M. K. Meyer, M. J. Kramer, and M. Akinc, Intermetallics **4**, 273 (1996).
2. M. K. Meyer and M. Akinc, J. Am. Ceram. Soc. **79** (10), 2763 (1996).
3. M. K. Meyer, A. J. Thom, and M. Akinc, Intermetallics **7**, 153 (1999).
4. M. Akinc, M. K. Meyer, M. J. Kramer, A. J. Thom, J. J. Heubsch, and B. Cook, Mater. Sci. Eng. **A261** (1-2), 16 (1999).
5. D. M. Berczik, United States Patent No. 5,595,616 (1997).
6. D. M. Berczik, United States Patent No. 5,693,156 (1997).
7. J. H. Schneibel, P. F. Tortorelli, M. J. Kramer, A. J. Thom, J. J. Kruzic, and R. O. Ritchie, in *Defect Properties and Related Phenomena in Intermetallic Alloys*, edited by E. P. George, M. J. Mills, H. Inui, and G. Eggeler (Materials Research Society, Warrendale, PA, 2003), Vol. 753, pp. 53-58.
8. J. H. Schneibel, R. O. Ritchie, J. J. Kruzic, and P. F. Tortorelli, Metall. Mater. Trans. **36A**, in press (2005).
9. J. J. Kruzic, J. H. Schneibel, and R. O. Ritchie, Scripta Mater. **50**, 459 (2004).
10. J. H. Schneibel, C. T. Liu, D. S. Easton, and C. A. Carmichael, Mater. Sci. Eng. **A261** (1-2), 78 (1999).
11. V Supatarawanich, D. R. Johnson, and C. T. Liu, Mater. Sci. Eng. **A344** (1-2), 328 (2003).
12. J. H. Schneibel, Intermetallics **11** (7), 625 (2003).
13. C. J. Gilbert, J. M. McNaney, R. H. Dauskardt, and R. O. Ritchie, J. Test. Eval. **22** (2), 117 (1994).
14. D. Chen, C. J. Gilbert, and R. O. Ritchie, J. Test. Eval. **28** (4), 236 (2000).
15. ASTM E647-00 in *Annual Book of ASTM Standards, Vol. 03.01: Metals- Mechanical Testing; Elevated and Low-temperature Tests; Metallography* (ASTM, West Conshohocken, Pennsylvania, USA, 2002), pp. 595-635.
16. K.T. Venkateswara Rao, W. O. Soboyejo, and R. O. Ritchie, Metall. Trans. **23A**, 2249 (1992).
17. I. Rosales and J. H. Schneibel, Intermetallics **8**, 885 (2000).
18. R. O. Ritchie, Int. J. Fract. **100** (1), 55 (1999).
19. H. Choe, D. Chen, J. H. Schneibel, and R. O. Ritchie, Intermetallics **9**, 319 (2001).
20. H. Choe, J. H. Schneibel, and R. O. Ritchie, Metall. Mater. Trans. **34A**, 25 (2003).